Inorganic Chemistry

Article

pubs.acs.org/IC

# $Cd^{2+}$ Triggered the FRET "ON": A New Molecular Switch for the Ratiometric Detection of $Cd^{2+}$ with Live-Cell Imaging and Bound X-ray Structure

Krishnendu Aich,[†] Shyamaprosad Goswami,*[,†] Sangita Das,[†] Chitrangada Das Mukhopadhyay,[‡] Ching Kheng Quah,[§] and Hoong-Kun Fun[§,∥]

[†]Department of Chemistry and [‡]Centre for Healthcare Science & Technology, Indian Institute of Engineering Science and Technology, Shibpur, Howrah-711 103, India

[§]X-ray Crystallography Unit, School of Physics, Universiti Sains Malaysia, 11800 USM, Penang, Malaysia

[∥]Department of Pharmaceutical Chemistry, College of Pharmacy, King Saud University, Riyadh 11451, Saudi Arabia

Supporting Information

**ABSTRACT:** On the basis of the Förster resonance energy transfer mechanism between rhodamine and quinoline−benzothiazole conjugated dyad, a new colorimetric as well as fluorescence ratiometric probe was synthesized for the selective detection of $Cd^{2+}$. The complex formation of the probe with $Cd^{2+}$ was confirmed through $Cd^{2+}$-bound single-crystal structure. Capability of the probe as imaging agent to detect the cellular uptake of $Cd^{2+}$ was demonstrated here using living RAW cells.

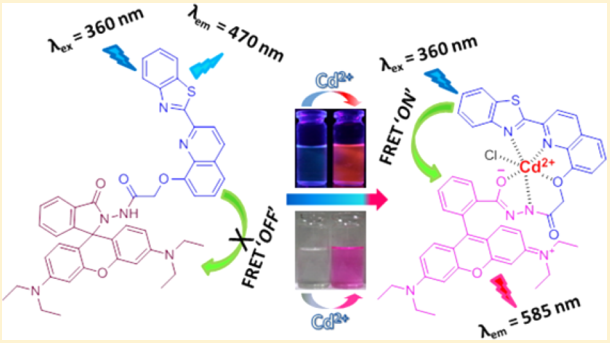


## INTRODUCTION

Heavy-metal contagion has become dangerous to the environment and human health.[1] Cadmium, a redundant element for life, is widely used in fertilizers and batteries, resulting in the widespread contamination of it in air, water, and soil.[2] It is not only a severe environmental hazard but also can pose serious health threats to humans.[3] $Cd^{2+}$ has been recognized as a highly toxic heavy metal ion and is enlisted by the U.S. Environmental Protection Agency, Disease Registry, and Agency for Toxic Substances as one of the superior pollutants.[4] This poisonous $Cd^{2+}$ may insert in human body or living beings through uptake of contaminated food, water, or inhalation of smoke (cigarette smoke). The exposure (may be long- or short-term) to $Cd^{2+}$ may cause renal dysfunction, calcium metabolism disorders, mutations, as well as an increased incidence of cancers.[5] Consequently, there are great needs for a sensitive method to quantify and recognize $Cd^{2+}$ in environmental samples as well as in the living cells as the cellular uptake and carcinogenic mechanisms of $Cd^{2+}$ are still poorly understood. In this regard, the fluorescence spectroscopy is a promising and powerful tool for sensing and imaging metal ions, and the development of fluorescence sensors/probes has attracted increasing attention of the researchers in the recent years.[6]

Only a few fluorescence probes for $Cd^{2+}$ have been reported to date,[7,8] and few of them are ratiometric.[8] The "OFF−ON" type or intensity-based probes are often induced by numerous issues, as the single-emission intensity experiences interference from a variety of analyte-independent factors, such as sample environment, sample concentration, bleaching, illumination intensity, optical path length, etc.[9] The ratiometric approach is one of the solutions to overcome these problems and ensure the reliability. Ratiometric sensors, in contrast, rely on the changes in the intensity of two emission bands upon interaction with analytes. Thus, the interference induced by the unknown local sensor concentration and the deviations in detection conditions can be reduced by using the ratio of emission intensities at two different wavelengths.[10]

In recent studies, Förster resonance energy transfer (FRET) is a widely used sensing mechanism for the design of fluorescence ratiometric probes. This nonradiative process involves the energy transfer between a pair of fluorophores that acts as energy donor and acceptor linked together through a nonconjugated spacer. The necessary requirements to show high FRET efficiency are a substantial overlap between the emission of the donor and absorption bands of the acceptor and an appropriate distance between the donor and acceptor (∼10−100 Å) as the energy transfer occurs through space.[11]

Because of its colorless and nonfluorescent nature in its spiro ring-closed form and, in contrast, the pink-red colored and strong fluorescence in the ring-opened form, rhodamine dye was hugely popular in the field of probe design across the past

**Received:** April 13, 2015
**Published:** July 20, 2015





DOI: 10.1021/acs.inorgchem.5b00784
*Inorg. Chem.* 2015, 54, 7309−7315

decade.[11−13] Rhodamine dye acts as a good acceptor fluorophore in a system exhibiting FRET mechanism. The characteristic emission of a rhodamine-based dye in the spiro ring-closed form is inhibited, and the FRET dyad shows only the emission of the donor. Consequently, the FRET process of the sysytem is prohibited, whereas, after reaction/complexation with relevant analyte, the spiro ring of the rhodamine dye opens, which gives a strong emission, consequently activating the FRET process "ON". Taking such advantage of the rhodamine dye, to date, a number of the rhodamine-based FRET sensors have been reported for different types of analytes.[11,13] To the best of our knowledge, there has yet been no report of FRET sensor for $Cd^{2+}$ based on a rhodamine platform.

Taking these factors into account and in continuation of our work[14] we present here the design, synthesis, and cation-sensing property of a new ratiometric fluorescent probe, possessing the FRET process. For the FRET process to take place, we linked quinoline-conjugated benzothiazole group with rhodamine B dye through a nonconjugated spacer. The quinoline−benzothiazole system acts in the dyad as donor fluorophore, whereas rhodamine dye acts as acceptor. The emission spectra of quinoline−benzothiazole group overlap significantly with the absorption spectra of the ring-opened rhodamine dye (Figure S1, Supporting Information). That means the transfer of energy from donor to acceptor is possible, and consequently a FRET process between them is also possible upon interaction with a specific analyte.

## RESULTS AND DISCUSSIONS

The probe (RQBT) was prepared on the basis of the route shown in Scheme 1. Compound 3 was synthesized by condensation reaction of compound 4 and 2-aminothiophenol in anhydrous *N,N*-dimethylformamide (DMF) using catalytic amount of *p*-toluene sulfonic acid (TSA). Now the reaction of ethyl chloroacetate with compound 3 in anhydrous DMF using potassium carbonate as base afforded compound 2, which reacts with hydrazine hydrate in refluxing methanol to yield compound 1. Formation of corresponding acid chloride from rhodamine B followed by reaction with compound 1 finally achieved the probe. Its chemical structure was well-characterized by $^1$H NMR, $^{13}$C NMR, and high-resolution mass spectrometry (HRMS; Figures S17−S25, Supporting Information). The structures of RQBT and its $Cd^{2+}$-bound complex were confirmed by single-crystal X-ray study. To the best of our knowledge, this is the first report of $Cd^{2+}$-bound crystal structure based on the rhodamine platform. Detailed synthetic procedure for the probe was provided in the Experimental Section.

**Scheme 1. Synthetic Procedure of the Probe RQBT**[a]

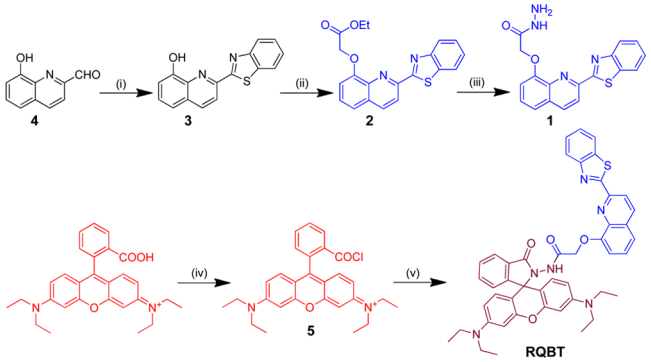


[a]Reagents and conditions: (i) 2-aminothiophenol, *p*-TSA, DMF, 60°−70° C, 12 h; (ii) ethyl chloroacetate, $K_2CO_3$, TBAB, DMF, rt, 12 h; (iii) $N_2H_4{\cdot}H_2O$, $CH_3OH$, reflux, 1 h; (iv) $POCl_3$, 1,2 dichloroethane, reflux, 4 h; (v) $CH_3CN$, $Et_3N$, reflux, 12 h.

To find out the effect of water content in the fluorogenic response of RQBT toward $Cd^{2+}$, we recorded the emission spectral changes of RQBT (10 $\mu$M) in different fractions of water−methanol mixture, followed by the addition of 3 equiv of $Cd^{2+}$. It was observed that up to 80% of water content in the RQBT-$Cd^{2+}$ solution, the probe was able to show modest emission in the intensity ratio at ($I_{585}/I_{470}$); above that, a decrease in the emission intensity was noticed. A comparative view of emission intensity change with the water content is shown in Supporting Information, Figure S8. To have good results and improved sensitivity, we used 80% aqueous methanol solution in the titration experiments.

All the UV−vis and fluorescence titrations of RQBT (10 $\mu$M) were conducted in MeOH/$H_2O$ (1/4, v/v, 1 mM HEPES buffer, pH = 7.2) solutions. As expected, the spirolactam ring of RQBT is not affected under this condition; consequently, the solution remains colorless. In the absorption spectra, RQBT (10 $\mu$M) itself exhibits three absorption bands at 262, 300, and 360 nm, but no peak appears at 565 nm, indicating the probe predominantly exits in spirolactam form (Figure 1a). Now, upon addition of $Cd^{2+}$, a distinct new peak having the maximum at 565 nm appeared, resulting in a visually detectable color change from colorless to pink (Figure 1a, inset). The

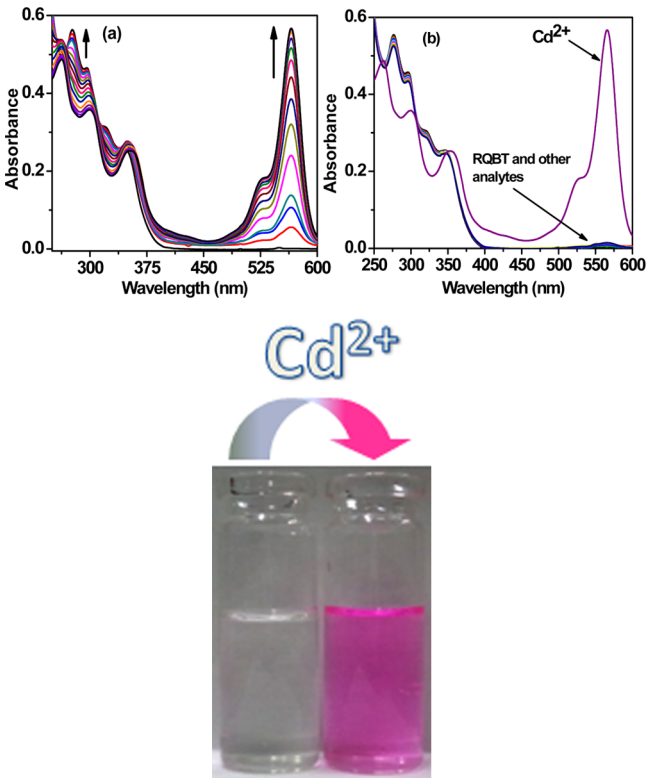


**Figure 1.** UV−vis spectra of RQBT (10 $\mu$M) in the presence of (a) $Cd^{2+}$ (0−3 equiv) and (b) different analytes (5 equiv). (inset) Visible color change of RQBT upon addition of 2 equiv of $Cd^{2+}$ in ambient light. All experiments were performed in MeOH/$H_2O$ (1/4, v/v, 1 mM HEPES buffer, pH = 7.2) media.



DOI: 10.1021/acs.inorgchem.5b00784
*Inorg. Chem.* 2015, 54, 7309−7315

intensity of the new peak at 565 nm gradually increases with incremental introduction of $Cd^{2+}$ (0−3 equiv) in RQBT solution. Now this observation eventually explains the opening of spirolactam form due to the complexation of RQBT with $Cd^{2+}$. The absorbance intensity of the probe RQBT at 565 nm increased linearly with the added $Cd^{2+}$ concentration in the range of 0−8 $\mu$M. Further increasing concentrations of $Cd^{2+}$ more than 1 equiv, the absorbance spectra exhibited no significant changes, and the intensity of absorption at 565 nm also reached to a plateau (Figure S2, Supporting Information).

The change in emission spectra of RQBT upon titration with $Cd^{2+}$ is depicted in Figure 2a. Irradiation of RQBT (10 $\mu$M) at

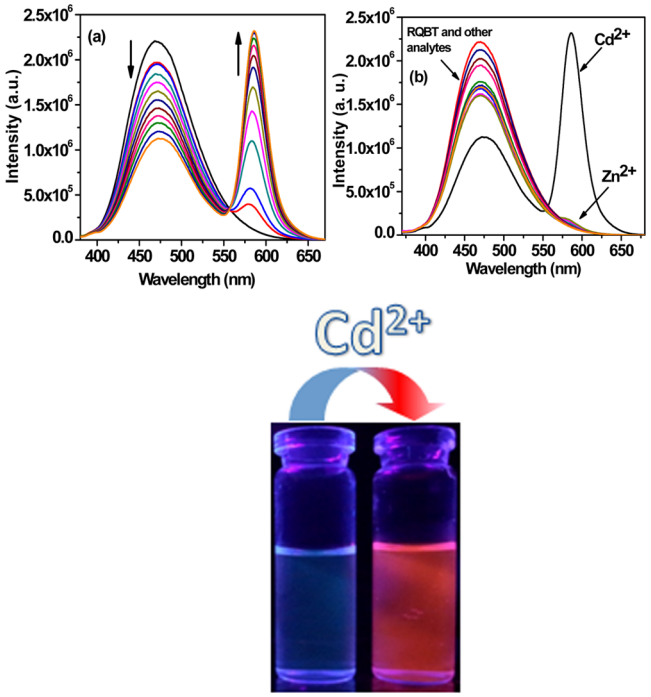


**Figure 2.** Emission spectra of RQBT (10 $\mu$M) in the presence of (a) $Cd^{2+}$ (0−3 equiv) and (b) different analytes (5 equiv). $\lambda_{ex}$ = 360 nm. (inset) Emission color change of RQBT upon addition of 2 equiv of $Cd^{2+}$ after illumination under UV light. All experiments were performed in MeOH/$H_2O$ (1/4, v/v, 1 mM HEPES buffer, pH = 7.2) media.

360 nm resulted in emission mainly from the donor component (quinoline−benzothiazole conjugated system) with a strong band centered at 470 nm, and no emission peak was observed at 585 nm, which strongly indicates stability of spirolactam network under this condition. This result also points out that, under this circumstance in absence of any guest analyte no energy transfer takes place from donor to acceptor system of RQBT. After addition of $Cd^{2+}$ a dramatic enhancement of fluorescence at 585 nm was observed, demonstrating the opening of the spiro ring. Upon incremental addition of $Cd^{2+}$ the peak at 470 nm gradually decreases, and the new peak at 585 nm increases readily exhibiting a beautiful ratiometric response. Meanwhile a clear isoemission point comes into view at 550 nm. The ratio of the emissions at the two wavelengths ($I_{585}/I_{470}$) increased from 0.054 to 2.07, after addition of 3 equiv of $Cd^{2+}$.

These experimental results are correlated well with the FRET process ON from the donor to the acceptor moiety (Scheme 2) of RQBT dyad after addition of $Cd^{2+}$. Consequently, the

**Scheme 2. Proposed FRET-Based Sensing Strategy of RQBT with $Cd^{2+}$**

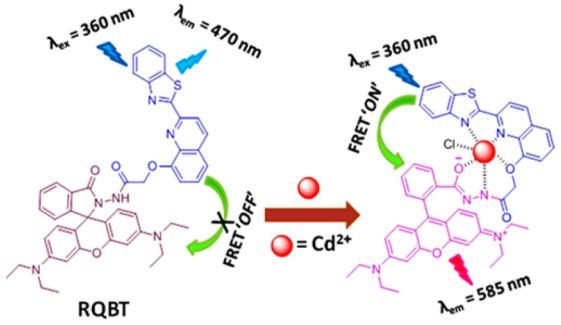


fluorescence of RQBT clearly changed from blue to red, which was easily detectable through naked eyes after illumination under UV light (Figure 2a, inset). The FRET efficiency of RQBT was calculated to be 48% (Supporting Information).

The fluorescence quantum yield of RQBT was evaluated as $\Phi$ = 0.26 (for $\lambda_{em}$ = 470 nm), whereas this value was changed to $\Phi$ = 0.37 (for $\lambda_{em}$ = 585 nm) after complexation with $Cd^{2+}$ (Supporting Information). During the course of addition of $Cd^{2+}$, the emission intensity ratio ($I_{585}/I_{470}$) of RQBT maintains a good linearity with the added $Cd^{2+}$ concentration from 0 to 9.5 $\mu$M (Figure S3b, Supporting Information) with an $R^2$ value of 0.996.

To find the limit of detection of $Cd^{2+}$ by the probe, that is, how lower amount (minimum concentration) of $Cd^{2+}$ can be estimated by the probe (RQBT), we recorded again fluorescence titration experiment. For this reason we recorded the data starting from the $Cd^{2+}$ concentration in the very low range ($1 \times 10^{-8}$ M) using 1 $\mu$M solution ($CH_3OH/H_2O$, 1/4, v/v, pH = 7.4, 1 mM HEPES buffer) of RQBT (Figure S9, Supporting Information). Hence from the fluorescence titration experiment it was found that minimum $2.7 \times 10^{-7}$ M $Cd^{2+}$ can develop the fluorescence intensity ratio ($I_{585}/I_{470}$) of RQBT. Thus, this is the lowest concentration of $Cd^{2+}$ detected by RQBT, so the detection limit of RQBT was found to be $2.7 \times 10^{-7}$ M for $Cd^{2+}$.

The association constant ($K_a$) of RQBT with $Cd^{2+}$ was determined using the nonlinear least-squares fit of the data obtained from fluorescence titration, and it was found to be $(1.23 \pm 0.17) \times 10^5$ $M^{-1}$ (Figure S10, Supporting Information).[15] We also determined the binding constant from the emission data in 95% buffer solution, and it was found to be $(1.87 \pm 0.15) \times 10^5$ $M^{-1}$ (Figure S11, Supporting Information).

Next, the selectivity and interference of RQBT to recognize $Cd^{2+}$ was evaluated. Common interfering metal ions ($K^+$, $Ca^{2+}$, $Ni^{2+}$, $Mn^{2+}$, $Zn^{2+}$, $Cu^{2+}$, $Fe^{3+}$, $Cr^{3+}$, $Hg^{2+}$, and $Pb^{2+}$) were tested for their ability to perturb the absorption and fluorescence behavior of RQBT. Only $Cd^{2+}$ is found to influence the spectral behavior of RQBT in both UV and fluorescence (Figures 1b and 2b). Competition experiment was also performed with the probe to estimate the effect of the detection of $Cd^{2+}$ in the presence of other guest cations. None of other ions of interest caused any significant change in the fluorescence spectra, which is mainly because of the stable complexation of RQBT with $Cd^{2+}$ ion (Figure S13, Supporting Information). Especially $Zn^{2+}$ and $Hg^{2+}$ do not significantly disturb the UV and fluorescence spectra of RQBT. The selectivity of the probe toward $Cd^{2+}$ may be explained on the basis of cavity space and the radii of the


DOI: 10.1021/acs.inorgchem.5b00784
Inorg. Chem. 2015, 54, 7309−7315

analyte of interest. For $Cd^{2+}$ there exists an exact fitting of the radii within the cavity, and a strong bond was formed by the $Cd^{2+}$ and the coordinating atoms, whereas $Zn^{2+}$ cannot fit that well to the cavity created by the binding zone. However, $Cd^{2+}$ with the perfect fitting radii can exactly fill the space and help FRET process to occur. Now the crystal structure established that the binding of RQBT toward $Cd^{2+}$ has beautifully happened by using N atom of benzothiazole moiety, N and O atoms of hydroxyquinoline, and N atom of the rhodamine−hydrazine moiety. These findings suggest that substituted 2-position of hydroxyquinoline by benzothiazole group is very favorable for binding with $Cd^{2+}$. A large cavity was found to form, which is highly favorable to accommodate $Cd^{2+}$. However, selectivity of the probe to detect $Cd^{2+}$ in comparison to $Zn^{2+}$ can be concluded that the complexation with $Zn^{2+}$ is absent of appropriate matching. Hence it may be concluded that, although $Cd^{2+}$ and $Zn^{2+}$ share a very similar characteristic, in this case $Cd^{2+}$ wins over $Zn^{2+}$.

To evaluate the pH sensitivity of RQBT, emission spectral study of the probe (10 $\mu$M) was also performed in mixed aqueous medium (MeOH/$H_2O$, 1/4, v/v) at varying solution of different pH, and the results showed that the conversion from spirocyclic to acyclic xanthene form of the probe could occur only at pH < 4 (Figure S12, Supporting Information). In basic pH the probe was found to be very stable, and no spectral change in the emission profile was observed. Thus, from the pH titration experiment we found that the probe is stable in the pH range from 12 to 4 and can be easily used in the system at near-neutral pH. The pH variation of the probe RQBT in the presence of $Cd^{2+}$ was also studied by means of fluorescence experiment. It was noticed that the detection of $Cd^{2+}$ was not affected in the basic, neutral region. The fluorescence intensity at 585 nm was almost unaltered within the pH < 4, but with decreasing pH (lower than 4) the detection of $Cd^{2+}$ was a little disturbed. The pH study exposed that the probe RQBT can sense $Cd^{2+}$ with almost no intervention in basic, near-neutral, and moderately acidic pH conditions.

X-ray analysis reveals that RQBT crystallizes in orthorhombic system with space group $Pna2_1$ with $a$ = 23.876 (5) Å, $b$ = 22.519 (4) Å, $c$ = 8.2710 (18) Å, $Z$ = 4, and $V$ = 4447.0 (16) Å$^3$, whereas RQBT with $Cd^{2+}$ crystallizes in triclinic system with space group $P\bar{1}$ with $a$ = 12.376(3) Å, $b$ = 14.329(4) Å, $c$ = 14.985(4) Å, $\alpha$ = 103.165(3)°, $\beta$ = 106.203(3)°, $\gamma$ = 108.041(3)°, $Z$ = 2, and $V$ = 2278.3(10) Å$^3$. The crystal structure of RQBT features for intramolecular N3—H1N3···N2 hydrogen bond producing an S(8) ring motif, which is assumed to contribute to the stability of the molecule (Figure 3a).

In RQBT-$Cd^{2+}$ the six-coordinate $Cd^{2+}$ atom exists in a distorted pentagonal pyramid geometry, coordinated by two N atoms from benzo[$d$]thiazole and quinoline, an O atom from benzamide, a N atom and an O atom from glycolamide, and additionally, a Cl atom (Figure 3b). The average values for the Cd−O and Cd−N bond distances are 2.505 and 2.314 Å, respectively. In RQBT (Figure 3a), the mean plane of isoindoline ring system forms dihedral angles of 88.96(17), 70.6(2), and 67.0(2)° with the xanthene, benzo[$d$]thiazole, and quinoline ring systems. The dihedral angle between benzo[$d$]-thiazole and quinoline ring systems is 6.3(3)° indicating these systems are almost coplanar to each other. The corresponding dihedral angles (benzene ring) are 58.2(4), 54.2(4), 45.8(4), and 8.7(3)° when RQBT binds with $Cd^{2+}$ (Figure 3b).

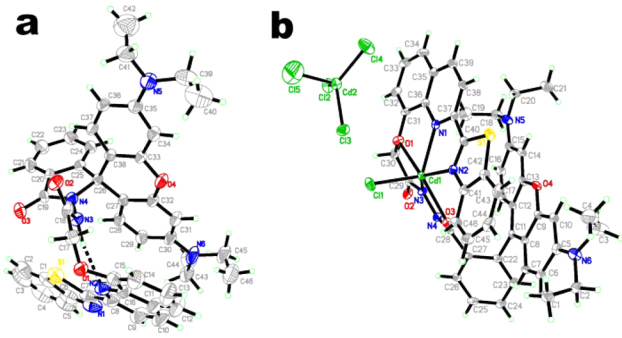


**Figure 3.** Crystal structures of (a) RQBT and (b) RQBT-$Cd^{2+}$, showing 30% probability displacement ellipsoids for non-H atoms and the atom-numbering scheme. Hydrogen bonds are represented by dashed lines.

In the crystal packing of RQBT (Figure S14), two hydrogen bonds via C23—H23A···O3 and C45—H45A···O2 (Table S2) are between the chains resulting in a two-dimensional net-shaped structure extending along the (100) plane with approximately rectangular grids of 8.271 × 11.707 Å. Short intermolecular distances between the centroids of the pyrrole with benzene rings (C27−C32 [3.827(3) Å] and C33−C38 [3.830(3) Å]) indicate the existence of weak $\pi\cdots\pi$ interactions. In the crystal structure of RQBT that binds with $Cd^{2+}$ (Figure S15), the tetrachlorocadmate molecules are linked to the main molecules into two-dimensional networks via C4—H4B···Cl5, C20—H20A···Cl2, and C30—H30B···Cl3 hydrogen bonds. The packing is further consolidated by C17—H17···O2 hydrogen bonds. Weak C−H···$\pi$ interactions are observed for both structures (Table S2).

The binding mode of the probe RQBT was depicted in Scheme 2. The binding ratio was established from the results of the HRMS data for the RQBT-$Cd^{2+}$ complex, which show a peak at $m/z$ 923.0558 possibly for $[M + Cd^{2+} + Cl^-]^+$, proves the mononuclear complex of RQBT with $Cd^{2+}$ (Figure S26, Supporting Information). The (1:1) stoichiometry between RQBT and $Cd^{2+}$ was further confirmed through single-crystal X-ray study of RQBT−$Cd^{2+}$ complex (Figure 3b). As per our knowledge, this $Cd^{2+}$-bound crystal on rhodamine platform is previously unknown. To establish the interaction of the probe toward $Cd^{2+}$ in solution state $^1$H NMR titration experiment was also performed with the probe RQBT in the existence of $Cd^{2+}$. From the $^1$H NMR it was noticed that a slight shift occurs in the aliphatic region of the $Cd^{2+}$−RQBT complex. Most prominent change noticed in $^1$H NMR titration study is the disappearance of NH (amide) peak in the $^1$H NMR data (Figure S27, Supporting Information). There is no peak at ∼9.94 ppm after addition of $Cd^{2+}$ indicating the complex formation takes place by N atom (N atom of amide). From the above findings it is clear that in solution state also the probable binding mode of the probe RQBT with $Cd^{2+}$ is similar to that in solid state (Scheme 2). Consideration of the practical application led to further examination of the ability of the probe (RQBT) to sense $Cd^{2+}$ in the living cells. We use here RAW 264.7 cells for the bioimaging application of RQBT.

The RAW 264.7 cells (Figure 4) were incubated with 10 $\mu$M RQBT for 30 min (37 °C), and the cells showed strong blue fluorescence and insignificant or weak red fluorescence (Figure 4a,b). Once the cells pretreated with RQBT were incubated with $CdCl_2$ (20 $\mu$M) for 30 min (37 °C) in the culture medium, a significant red fluorescence was observed from the



DOI: 10.1021/acs.inorgchem.5b00784
*Inorg. Chem.* 2015, 54, 7309−7315

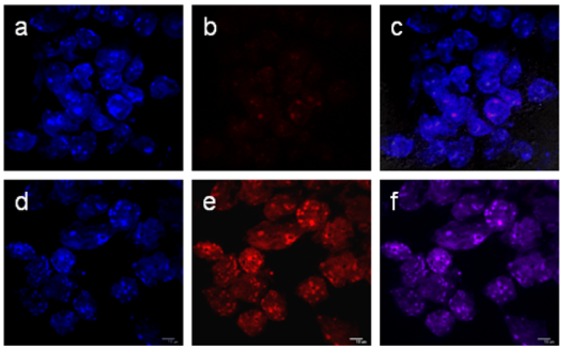


**Figure 4.** Confocal fluorescence images of RAW 264.7 cells incubated with 10 $\mu$M of RQBT for 20 min (a, b) and then 20 $\mu$M of $CdCl_2$ for 10 min (d, e). All images were obtained using 360 nm excitation and emission channels of (a, d) 450−480 nm (blue) and (b, e) 570−600 nm (red). (c) Merged image of (a) and (b). (f) Merged image of (d) and (e). Scale bar = 10 $\mu$m. pH of the media were maintained at 7.4 using HEPES (10 mM) buffer.

intracellular area along with a weak blue fluorescence (Figure 4d,e). RQBT is particularly useful for imaging of biological samples for its permeability as well as stability in neutral pH. This fluorescent probe is easily taken up by the cells without causing any damage such as lysis or swelling.

Cell viability assay was also performed, and it is given in Figure S16 (Supporting Information). This experiment shows that RQBT is nontoxic to living cells. These results suggest that the probe, RQBT, was cell-membrane permeable and could be used as a chemosensor to detect $Cd^{2+}$ in living cells.

Motivated by the favorable rapid sensing of RQBT toward $Cd^{2+}$, we took a step forward toward the potential application by using it as a portable kit for sensing $Cd^{2+}$. This experiment is very easy but very important, because without any instrumental help it can give instant qualitative information. Now to carry out this experiment we arranged thin-layer chromatography (TLC) plates that were immersed into the solution of RQBT ($2 \times 10^{-4}$ M) in MeOH and then kept the TLC plate in air for few minutes to evaporate the solvent to dryness, followed by immersing the TLC plate to $Cd^{2+}$ ($2 \times 10^{-3}$ M) solution and then again evaporation of the solvent in air. The color of the TLC plate changes from colorless to pink and blue to bright red under ambient light and hand-held UV light, respectively (Figure 5).

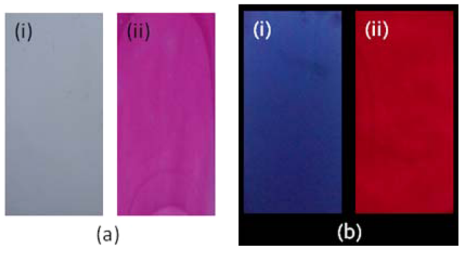


**Figure 5.** Photographs of TLC plates after immersion in an RQBT−MeOH solution (i) and after immersion in an RQBT−$Cd^{2+}$ methanol solution (ii) taken in ambient light (a) and under hand-held UV light (b). Excitation wavelength of the UV light is 365 nm. [RQBT] = $2 \times 10^{-4}$ M and [$Cd^{2+}$] = $2 \times 10^{-3}$ M.

## CONCLUSION

In conclusion, herein we report the synthesis of a new probe based on rhodamine dye, conjugated with quinoline−benzothiazole moiety, which showed a specific colorimetric and fluorescence ratiometric response upon binding with $Cd^{2+}$ through turn on the FRET process. The single-crystal X-ray structures of both the probe and its $Cd^{2+}$ bound complex are reported as proof of binding. The nontoxicity of the probe makes it useful as an imaging agent for the detection of $Cd^{2+}$ in living cells.

## EXPERIMENTAL SECTION

**General.** The materials used for this study were obtained from Sigma-Aldrich and used without further purification. Merck 60 $F_{254}$ plates with a thickness of 0.25 mm were used for TLC. $^1H$ and $^{13}C$ NMR spectra were recorded on Bruker 500/400 MHz instruments and mentioned in the figure captions of the NMR spectra. $CDCl_3$ or deuterated dimethyl sulfoxide (DMSO-$d_6$) were used as solvent for NMR spectra using tetramethylsilane as an internal standard. UV−vis spectra were recorded on a JASCO V-630 spectrometer. Fluorescence spectra were recorded on Photon Technology International fluorescence spectrometer. For the titration experiment we used the cations (metal ions) $Na^+$, $K^+$, $Ca^{2+}$, $Ni^{2+}$, $Mn^{2+}$, $Zn^{2+}$, $Cd^{2+}$, $Cu^{2+}$, $Fe^{3+}$, $Mg^{2+}$, $Cr^{3+}$ and $Pb^{2+}$ as their chloride salts.

**Synthesis of [2-(Benzo[*d*]thiazol-2-yl)quinolin-8-ol] Compound 3.** Compound 4 (0.5 g, 2.89 mmol) and 2-aminothiophenol (0.43 g, 3.44 mmol) were dissolved together in DMF (4 mL). A catalytic amount of *p*-TSA was added to it, and the mixtures were stirred at 60−70 °C under $N_2$ atmosphere for 12 h. After it cooled to room temperature (rt), the brownish-red solution was poured into ice water with continuous stirring. Brownish-yellow precipitate separated out, which was filtered, washed with water, and dried in vacuum. The crude product was purified through column chromatography using petroleum ether/ethyl acetate (9/1, v/v) as eluent to give the yellow solid as pure compound (0.62 g, 78%). $^1H$ NMR (400 MHz, $CDCl_3$): $\delta$ 7.27 (m, 1H), 7.39 (d, $J$ = 8 Hz, 1H), 7.46 (t, $J$ = 6 Hz, 1H), 7.54 (m, 2H), 7.98 (dd, 1H), 8.08 (s, 1H), 8.15 (d, $J$ = 8 Hz, 1H), 8.31 (d, $J$ = 6.8 Hz, 1H), 8.52 (d, $J$ = 8 Hz, 1H). HRMS: calculated for $C_{16}H_{11}N_2OS$ $[M + H]^+$ ($m/z$): 279.0592; found:279.0589.

**Synthesis of [Ethyl 2-((2-(benzo[*d*]thiazol-2-yl)quinolin-8-yl)oxy)acetate] Compound 2.** The mixture of compound 3 (0.5 g, 1.79 mmol) and $K_2CO_3$ (0.5 g, 3.64 mmol) in DMF (5 mL) under $N_2$-atmosphere was stirred for 10 min at rt before addition of ethylchloroacetate (0.33 g, 2.70 mmol). Catalytic amounts of KI and tetra-*n*-butylammonium bromide (TBAB) were added successively to the reaction mixture, which was left stirring for 12 h at rt. After the starting material was consumed as indicated by TLC, the whole mixture was poured into ice−water (10 mL) and then extracted with dichloromethane (DCM, 3 × 15 mL). All the organic parts were collected and dried over anhydrous $Na_2SO_4$, and the solvent was evaporated to get the crude product. The residue was subjected to column chromatography using petroleum ether/ethyl acetate (4/1, v/v) as eluent to afford the pure compound as white solid (0.53 mg, 82%). $^1H$ NMR (400 MHz, $CDCl_3$): $\delta$ 1.36 (t, $J$ = 5.6 Hz, 3H), 4.34 (q, $J$ = 5.8 Hz, 2H), 5.08 (s, 2H), 7.17 (dd, 1 H), 7.44 (t, $J$ = 6 Hz, 1H), 7.51 (m, 3H), 7.97 (d, $J$ = 6.4 Hz, 1H), 8.13 (d, $J$ = 6.8 Hz, 1H), 8.29 (d, $J$ = 6.8 Hz, 1H), 8.52 (d, $J$ = 6.4 Hz, 1H). HRMS: calculated for $C_{20}H_{17}N_2O_3S$ $[M + H]^+$ ($m/z$): 365.0960; found: 365.1420.

**Synthesis of [2-((2-(Benzo[*d*]thiazol-2-yl)quinolin-8-yl)oxy)-acetohydrazide] Compound 1.** $N_2H_4{\cdot}H_2O$ (excess) was added to the solution of compound 2 (0.25 g, 0.68 mmol) in methanol (10 mL). The mixture was stirred for 1 h in refluxing condition. After it cooled at rt, the solvent was evaporated under reduced pressure, and the residue was poured onto ice−water. White precipitate appeared, which was filtered and dried in vacuum. The compound is pure enough and used directly for the next step without further purification. $^1H$ NMR (500 MHz, DMSO-$d_6$): $\delta$ 4.49 (s, 2H), 4.88 (s, 2H), 7.34 (d, $J$ = 8 Hz, 1H), 7.53 (t, $J$ = 7.5 Hz, 1H), 7.61 (m, 2H), 7.68 (d, $J$ = 8



DOI: 10.1021/acs.inorgchem.5b00784
*Inorg. Chem.* 2015, 54, 7309−7315

Hz, 1H), 8.15 (d, $J$ = 8 Hz, 1H), 8.20 (d, $J$ = 8 Hz, 1H), 8.47 (d, $J$ = 8.5 Hz, 1H), 8.57 (d, $J$ = 8.5 Hz, 1H), 9.34 (s, 1H). HRMS: calculated for $C_{18}H_{14}N_4NaO_2S$ $[M + Na]^+$ ($m/z$): 373.0735; found: 373.0732.

**Synthesis of the Probe (RQBT).** To a solution of rhodamine B (0.5 g, 1.04 mmol) in 1,2-dichloroethane (15 mL), phosphorus oxychloride (1.0 mL) was added dropwise over 2 min. The solution was refluxed for 4 h. The reaction mixture was cooled to rt and evaporated to give rhodamine B acid chloride, which was directly used in the next step without purification. A solution of compound 1 (0.38 g, 1.08 mmol) and triethylamine (3 mL) in acetonitrile (10 mL) was added dropwise to the acetonitrile (15 mL) solution of crude acid chloride. The reaction mixture was refluxed for 12 h under $N_2$ atmosphere. After the mixture cooled to rt, followed by evaporation of the solvent, water (10 mL) was added to the crude product and was then extracted with DCM (3 × 20 mL). The combined organic portions were dried over the anhydrous sodium sulfate. After evaporation of the solvent under reduced pressure, the crude pink solid was purified through column chromatography using DCM as eluent to afford RQBT (0.47 g, 58%) as yellow solid. $^1$H NMR (400 MHz, $CDCl_3$): $\delta$ 1.00 (t, $J$ = 7.2 Hz, 12H), 3.16 (q, $J$ = 6.8 Hz, 8H), 4.83 (s, 2H), 5.92 (s, 2H), 6.00 (dd, $J$ = 8.8 Hz, 2H), 6.48 (d, $J$ = 8.8 Hz, 2H), 6.95 (d, $J$ = 7.6 Hz, 1H), 7.04 (q, $J$ = 5.6 Hz, 1H), 7.47 (m, 6H), 7.96 (d, $J$ = 8 Hz, 1H), 8.01 (d, $J$ = 8 Hz, 1H), 8.06 (d, $J$ = 8 Hz, 1H), 8.23 (d, $J$ = 8.4 Hz, 1H), 8.40 (d, $J$ = 8.4 Hz, 1H), 8.97 (s, 1H). $^{13}$C NMR (125 MHz, $CDCl_3$): $\delta$ 14.1, 44.2, 66.4, 69.4, 97.3, 104.4, 107.7, 112.5, 118.9, 121.4, 122.2, 123.6, 123.8, 124.2, 125.9, 126.2, 127.8, 128.1, 128.3, 129.3, 129.6, 130.1, 133.1, 136.7, 139.9, 148.7, 150.3, 151.3, 153.6, 153.7, 154.4, 164.9, 166.6, 169.9. HRMS: calculated for $C_{46}H_{43}N_6O_4S$ $[M + H]^+$ ($m/z$): 775.3066; found: 775.3062.

**$Cd^{2+}$ Complex of RQBT.** The receptor, RQBT (50 mg), and $CdCl_2$ (14 mg) were mixed together and dissolved in 5 mL of methanol. After reflux for 12 h the reaction mixture was cooled to rt. A red colored precipitate appeared, which was filtered and dried in vacuum. HRMS (electrospray ionization, positive): calcd. for $C_{46}H_{42}CdClN_6O_4S$ $[M + Cd^{2+} + Cl^-]^+$ ($m/z$): 923.1710; found: 923.0558.

**Method of Crystallization of RQBT.** RQBT (25 mg) was dissolved in DCM/$CH_3CN$ (1/1, v/v) in a conical flask, and it was allowed to stand in a cool place without any perturbation. After 3 d, diffraction-quality pink, block-shaped single crystals were separated out, and these were collected for X-ray crystallographic work.

**Method of Crystallization of RQBT-$Cd^{2+}$ Complex.** RQBT-$Cd^{2+}$ complex (20 mg) was dissolved in (DCM/$CH_3CN$/MeOH) solvent mixture in a conical flask, and it was allowed to stand in a cool place without any perturbation. After 6 d, diffraction-quality black, block-shaped single crystals were separated out, and these were collected for X-ray crystallographic work.

**Bioimaging Details.** *Materials and Methods.* Frozen human colorectal carcinoma cell line HCT 116 (ATCC:CCL-247) was obtained from the American Type Culture Collection (Rockville, MD) and maintained in Dulbecco's modified Eagle's medium (DMEM, Sigma Chemical Co., St. Louis, MO) supplemented with 10% fetal bovine serum (Invitrogen), penicillin (100 $\mu$g/mL), and streptomycin (100 $\mu$g/mL). The RAW 264.7 macrophages were obtained from NCCS, Pune, India, and maintained in DMEM containing 10% (v/v) fetal calf serum and antibiotics in a $CO_2$ incubator. Cells were initially propagated in 25 cm$^2$ tissue culture flask in an atmosphere of 5% $CO_2$ and 95% air at 37 °C humidified air until 70−80% confluency.

*Fluorescence Imaging Studies.* For fluorescence imaging studies, RAW cells, 7.5 × 10$^3$ cells in 150 $\mu$L of media were seeded on sterile 12 mm diameter poly-L-lysine-coated coverslip and kept in a sterile 35 mm covered Petri dish and incubated at 37 °C in a $CO_2$ incubator for 24−30 h. Next day cells were washed three times with HEPES (pH 7.4) and fixed using 4% paraformaldehyde in HEPES (pH 7.4) for 10 min at rt washed with HEPES followed by permeabilization using 0.1% saponin for 10 min. Then the cells were incubated with 10 $\mu$M of the probe (RQBT) dissolved in 100 $\mu$L of DMEM at 37 °C for 1 h in a $CO_2$ incubator and observed under epifluorescence microscope (Carl Zeiss). The cells were again washed thrice with HEPES (pH 7.4) to remove any excess probe and incubated in DMEM containing $CdCl_2$ (20 $\mu$M) followed by washing with HEPES (pH 7.4) three times to remove excess free metal ion outside the cells. Again, images were taken using epifluorescence microscope. Before fluorescence imaging, all the solutions were aspirated, and the samples were mounted on slides in a mounting medium and stored in dark before microscopic images were acquired.

## ■ ASSOCIATED CONTENT

### Ⓢ Supporting Information

Calculation of FRET efficiency, determination of detection limit, association constant, and quantum yield, pH study, competition study, characterization data for all newly synthesized compounds, NMR and HRMS spectra, X-ray data, bioimaging details, UV−vis and fluorescence data, additional references. The Supporting Information is available free of charge on the ACS Publications website at DOI: 10.1021/acs.inorgchem.5b00784.

## ■ AUTHOR INFORMATION

### Corresponding Author

*E-mail: spgoswamical@yahoo.com.

### Notes

The authors declare no competing financial interest.

## ■ ACKNOWLEDGMENTS

Authors thank the CSIR and DST, Government of India, for financial support. K.A. and S.D. acknowledge the CSIR for providing them fellowships. C.K.Q. and H.K.F. thank Universiti Sains Malaysia for Research University Individual Grant (No. 1001/PFIZIK/811278). The authors extend their appreciation to The Deanship of Scientific Research at King Saud University for the Research Group Project No. RGP VPP-207.

## ■ REFERENCES

(1) Zhuang, P.; McBride, M.; Xia, H.; Li, N.; Li, Z. *Sci. Total Environ.* **2009**, *407*, 1551.

(2) Taylor, M. D. *Sci. Total Environ.* **1997**, *208*, 123.

(3) (a) Järup, L.; Berglund, M.; Elinder, C. G.; Nordberg, G.; Vahter, M.; Teppo, L. *Scand. J. Work, Environ. Health* **1998**, *24*, 1. (b) Mendes, A. M. S.; Duda, G. P.; do Nascimento, C. W. A.; Silva, M. O. *Sci. Agric.* **2006**, *63*, 328.

(4) Agency for Toxic Substances and Disease Registry, Atlanta, GA. Online: http://www.atsdr.cdc.gov/cercla/07.

(5) Friberg, L.; Elinger, C. G.; Kjellström, T. *Cadmium;* World Health Organization: Geneva, Switzerland, 1992.

(6) (a) de Silva, A. P.; Gunaratne, H. Q. N.; Gunnlaugsson, T.; Huxley, A. J. M.; McCoy, C. P.; Rademacher, J. T.; Rice, T. E. *Chem. Rev.* **1997**, *97*, 1515. (b) Burdette, S. C.; Lippard, S. J. *Coord. Chem. Rev.* **2001**, *216-217*, 333.

(7) (a) Kim, H. N.; Ren, W. X.; Kim, J. S.; Yoon, J. *Chem. Soc. Rev.* **2012**, *41*, 3210. (b) Xu, L.; He, M.-L.; Yang, H.-B.; Qian, X. *Dalton Trans.* **2013**, *42*, 8218. (c) Xu, Y.; Xiao, L.; Sun, S.; Pei, Z.; Pei, Y.; Pang, Y. *Chem. Commun.* **2014**, *50*, 7514. (d) Goswami, S.; Aich, K.; Das, S.; Das, A. K.; Manna, A.; Halder, S. *Analyst* **2013**, *138*, 1903. (e) Goswami, S.; Aich, K.; Sen, D. *Chem. Lett.* **2012**, *41*, 863. (f) Yang, Y.; Cheng, T.; Zhu, W.; Xu, Y.; Qian, X. *Org. Lett.* **2011**, *13*, 264. (g) Liu, X.; Zhang, N.; Zhou, J.; Chang, T.; Fang, C.; Shangguan, D. *Analyst* **2013**, *138*, 901. (h) Wang, W.; Wen, Q.; Zhang, Y.; Fei, X.; Li, Y.; Yang, Q.; Xu, X. *Dalton Trans.* **2013**, *42*, 1827. (i) Zhang, L.; Hu, W.; Yu, L.; Wang, Y. *Chem. Commun.* **2015**, *51*, 4298. (j) Goswami, S.; Aich, K.; Das, S.; Mukhopadhyay, C. D.; Sarkar, D.; Mondal, T. K. *Dalton Trans.* **2015**, *44*, 5763. (k) Li, Y.; Chong, H.; Meng, X.; Wang, S.; Zhu, M.; Guo, Q. *Dalton Trans.* **2012**, *41*, 6189. (l) Ye, W.; Wang, S.; Meng, X.; Feng, Y.; Sheng, H.; Shao, Z.; Zhu, M.; Guo, Q. *Dyes Pigm.* **2014**, *101*, 30.



DOI: 10.1021/acs.inorgchem.5b00784
*Inorg. Chem.* 2015, 54, 7309−7315

(8) (a) Xue, L.; Li, G.; Liu, Q.; Wang, H.; Liu, C.; Ding, X.; He, S.; Jiang, H. *Inorg. Chem.* **2011**, *50*, 3680. (b) Tan, Y.; Gao, J.; Yu, J.; Wang, Z.; Cui, Y.; Yang, Y.; Qian, G. *Dalton Trans* **2013**, *42*, 11465. (c) Zhang, L.-K.; Tong, Q.-X.; Shi, L.-J. *Dalton Trans.* **2013**, *42*, 8567. (d) Shi, Z.; Han, Q.; Yang, L.; Yang, H.; Tang, X.; Dou, W.; Li, Z.; Zhang, Y.; Shao, Y.; Guan, L.; Liu, W. *Chem. - Eur. J.* **2015**, *21*, 290.
(9) Zhao, Q.; Li, F.; Huang, C. *Chem. Soc. Rev.* **2010**, *39*, 3007.
(10) Sapsford, K. E.; Berti, L.; Medintz, I. L. *Angew. Chem., Int. Ed.* **2006**, *45*, 4562.
(11) (a) Fan, J.; Hu, M.; Zhan, P.; Peng, X. *Chem. Soc. Rev.* **2013**, *42*, 29. (b) Yuan, L.; Lin, W.; Zheng, K.; Zhu, S. *Acc. Chem. Res.* **2013**, *46*, 1462. (c) Chen, B.; Wang, P.; Jin, Q.; Tang, X. *Org. Biomol. Chem.* **2014**, *12*, 5629.
(12) (a) Chen, X.; Pradhan, T.; Wang, F.; Kim, J. S.; Yoon, J. *Chem. Rev.* **2012**, *112*, 1910. (b) Zhou, L.; Zhang, X.; Wang, Q.; Lv, Y.; Mao, G.; Luo, A.; Wu, Y.; Wu, Y.; Zhang, J.; Tan, W. *J. Am. Chem. Soc.* **2014**, *136*, 9838. (c) Sun, S.; Qiao, B.; Jiang, N.; Wang, J.; Zhang, S.; Peng, X. *Org. Lett.* **2014**, *16*, 1132. (d) Reddy, G. U.; Ali, F.; Taye, N.; Chattopadhyay, S.; Das, A. *Chem. Commun.* **2015**, *51*, 3649. (e) Goswami, S.; Das, S.; Aich, K.; Sarkar, D.; Mondal, T. K.; Quah, C. K.; Fun, H.-K. *Dalton Trans.* **2013**, *42*, 15113. (f) Goswami, S.; Das, S.; Aich, K.; Nandi, P. K.; Ghoshal, K.; Quah, C. K.; Bhattacharyya, M.; Fun, H.-K.; Abdel-Aziz, H. A. *RSC Adv.* **2014**, *4*, 24881. (g) Zhu, H.; Fan, J.; Lu, J.; Hu, M.; Cao, J.; Wang, J.; Li, H.; Liu, X.; Peng, X. *Talanta* **2012**, *93*, 55.
(13) (a) Zhou, X.; Wu, X.; Yoon, J. *Chem. Commun.* **2015**, *51*, 111. (b) Hu, F.; Zheng, B.; Wang, D.; Liu, M.; Du, J.; Xiao, D. *Analyst* **2014**, *139*, 3607. (c) Chen, W.-D.; Gong, W.-T.; Ye, Z.-Q.; Lin, Y.; Ning, G.-L. *Dalton Trans.* **2013**, *42*, 10093. (d) Xuan, W.; Cao, Y.; Zhou, J.; Wang, W. *Chem. Commun.* **2013**, *49*, 10474. (e) Chereddy, N. R.; Thennarasu, S.; Mandal, A. B. *Analyst* **2013**, *138*, 1334. (f) Kumar, N.; Bhalla, V.; Kumar, M. *Analyst* **2014**, *139*, 543. (g) Wang, S.; Meng, X.; Zhu, M. *Tetrahedron Lett.* **2011**, *52*, 2840.
(14) (a) Goswami, S.; Das, S.; Aich, K.; Pakhira, B.; Panja, S.; Mukherjee, S. K.; Sarkar, S. *Org. Lett.* **2013**, *15*, 5412. (b) Goswami, S.; Aich, K.; Das, S.; Das, A. K.; Sarkar, D.; Panja, S.; Mondal, T. K.; Mukhopadhyay, S. K. *Chem. Commun.* **2013**, *49*, 10739. (c) Goswami, S.; Aich, K.; Das, A. K.; Manna, A.; Das, S. *RSC Adv.* **2013**, *3*, 2412. (d) Goswami, S.; Das, S.; Aich, K.; Sarkar, D.; Mondal, T. K. *Tetrahedron Lett.* **2013**, *54*, 6892. (e) Goswami, S.; Aich, K.; Das, S.; Roy, S. B.; Pakhira, B.; Sarkar, S. *RSC Adv.* **2014**, *4*, 14210. (f) Goswami, S.; Aich, K.; Das, S.; Pakhira, B.; Ghoshal, K.; Quah, C. K.; Bhattacharyya, M.; Fun, H.-K.; Sarkar, S. *Chem. - Asian J.* **2015**, *10*, 694. (g) Aich, K.; Goswami, S.; Das, S.; Mukhopadhyay, C. D. *RSC Adv.* **2015**, *5*, 31189. (h) Goswami, S.; Das, S.; Aich, K. *Tetrahedron Lett.* **2013**, *54*, 4620. (i) Goswami, S.; Das, S.; Aich, K. *RSC Adv.* **2015**, *5*, 28996.
(15) (a) Thordarson, P. *Chem. Soc. Rev.* **2011**, *40*, 1305. (b) Valeur, B.; Pouget, J.; Bourson, J.; Kaschke, M.; Ernsting, N. P. *J. Phys. Chem.* **1992**, *96*, 6545. (c) Ghosh, K.; Kar, D.; Sahu, D.; Ganguly, B. *RSC Adv.* **2015**, *5*, 46608.



DOI: 10.1021/acs.inorgchem.5b00784
*Inorg. Chem.* 2015, 54, 7309−7315